



Sorption of stable and radioactive Cs(I), Sr(II), Co(II) ions on Ti–Ca–Mg phosphates

Andrei Ivanets¹ · Vitaliy Milyutin² · Irina Shashkova¹ · Natalja Kitikova¹ · Natalya Nekrasova² · Artsiom Radkevich³

Received: 10 January 2020 / Published online: 19 April 2020
© Akadémiai Kiadó, Budapest, Hungary 2020

Abstract

In this paper, we studied the features of stable and radioactive Cs(I), Sr(II) and Co(II) ions sorption on Ti–Ca–Mg phosphates. The significant differences in the sorption of macro quantities of stable Cs⁺, Sr²⁺ and Co²⁺ ions and trace concentrations of ¹³⁷Cs, ⁹⁰Sr and ⁶⁰Co radionuclides were found. It has to be taken into account for evaluation the effectiveness of sorbents for the treatment of real liquid radioactive waste. Comparative studies with industrial sorbents have shown that the synthesized in this study mixed Ti–Ca–Mg phosphates are promising materials for one-stage treatment of liquid radioactive waste with complex chemical and radionuclide composition.

Keywords Liquid radioactive waste · Cs(I) · Sr(II) · Co(II) · Radionuclides · Ti–Ca–Mg phosphates · Adsorption

Introduction

The progress in use of nuclear power, sources of ionizing radiation is inextricably linked to the generation and accumulation of liquid radioactive waste (LRW), which demands the development of new effective technologies and materials for their safe management. One of the most important problems of LRW treatment is selective extraction of long-lived radionuclides ¹³⁷Cs, ⁹⁰Sr, and ⁶⁰Co [1–3]. Precipitation and coagulation methods are widely used for removing of easily hydrolyzed radionuclides or formation of poorly soluble carbonate compounds [4, 5]. Ion exchange is effective in removing radionuclides that are not prone to complexation and are present in solution as hydrated ions [6, 7]. Membrane methods can be applied at various stages of LRW processing alone or in combination with other methods. For example,

micro- and ultrafiltration demonstrate high efficiency when combined with precipitation/coagulation [8]. Nanofiltration and reverse osmosis make it possible to remove a wide range of radionuclides in a soluble form, which leads to a wider application of these methods [9].

A special place among the above methods is occupied by sorption, due to the possibility of selective removal of individual radionuclides from LRW with complex chemical and radionuclide composition. The choice of the treatment method depends on many factors: the composition of the LRW, pH, the presence of competing ions, complexing reagents, surfactants etc. Therefore, many publications devoted to sorption treatment of LRW are focused on the influence of the above listed factors on the efficiency of radionuclides removal [10–13].

The state and radionuclide species in solution is one of the most important characteristics that should be taken into account when planning the experiment and interpreting the results [14]. Given the complexity of handling radionuclides in the laboratory, stable isotopes are often chosen for the preparation of model solutions. At the same time, the concentration of stable ions in model solutions significantly exceeds the content of radionuclides in real medium- and low-level activity LRW. In case of stable ions, the sorption capacity and removal degree values are used as criteria for evaluating the effectiveness of the studied materials [15–18]. In the case of radionuclides, the values of the distribution coefficient and the separation

✉ Andrei Ivanets
ivanets@igic.bas-net.by; andreiivanets@yandex.ru

¹ Institute of General and Inorganic Chemistry of the National Academy of Sciences of Belarus, St. Surganova 9/1, 220072 Minsk, Belarus

² A.N. Frumkin Institute of Physical Chemistry and Electrochemistry of the Russian Academy of Sciences, Bld.4 31 Leninsky Prospekt, Moscow, Russia 199071

³ Joint Institute for Power and Nuclear Research, Sosny of the National Academy of Sciences of Belarus, PO Box 119, 220109 Minsk, Belarus

coefficient are calculated [19–22]. In terms of chemical behavior under the same conditions, stable and radioactive elements behave the same way. However, it is important to take into account that the behavior of various chemical compounds in sorption processes, in particular metal ions Cs(I), Sr(II) and Co(II), can significantly depend on their concentration in solution. For low- and medium-level liquid radioactive waste, the content of radionuclides is located in the area of micro-concentrations, and we are dealing with “trace” amounts of radionuclides. In this case, the sorption of metals occurs at the initial site of the isotherm (the area in which Henry’s law is fulfilled). For this reason, it is not the total number of ionogenic groups that is crucial, as in the case of sorption of macro-quantities, but the state of the surface ionogenic centers that determine the specificity and affinity for the extracted radionuclide ion.

Other specific feature of radionuclide behavior in trace concentrations in solution is the formation of pseudo-colloids. These species are formed either from a phase that does not include the element of interest, but which have sequestered the element, incorporated or on the surface. Conditions for pseudo-colloids existence may vary significantly depending on solution composition and the transition of radionuclides from ionic to non-ionic species influences their sorption properties [23, 24].

Previously, we were the first to synthesize composite materials based on mixed Ti–Ca–Mg phosphates from dolomite as a natural raw material and titanyl-diammonium sulfate synthesized from waste products of apatit-nefelin ores. The high efficiency of the obtained sorbents was shown in model LRW treatment containing a mixture of ^{137}Cs , ^{90}Sr and ^{60}Co radionuclides [25]. Vary the ratio of Ti/(Ca–Mg) in phosphate sorbents allows to change selectivity to each of the radionuclides. The use of broad-spectrum sorbents allows for one-stage removal of the above-mentioned radionuclides, which greatly simplifies the technology of LRW processing. It has been shown that the prevailing mechanism of the Cs^+ is ion-exchange due to the presence of the titanium hydrophosphate phase during the study of the sorption properties of the obtained novel sorbent towards Cs^+ , Sr^{2+} and Co^{2+} cations. A synergistic effect of individual phosphates has been observed for the Sr^{2+} and Co^{2+} removal. The sorption proceeds according to the precipitation mechanism of low soluble phosphates of cobalt and strontium, surface complexation, and the ion-exchange mechanism. It should be noted that the sorption capacity of a composite sorbent is due to the chemical composition of the final solid phase [26]. It is obvious that established differences in sorption mechanism of Cs^+ , Sr^{2+} and Co^{2+} ions determine the importance of conducting research on sorption for stable ions and radionuclides for evaluating the effectiveness of various sorbents for real LRW treatment.

The objective of this work is to study the features of stable Cs^+ , Sr^{2+} and Co^{2+} ions and radioactive ^{137}Cs , ^{90}Sr and ^{60}Co isotopes sorption on Ti–Ca–Mg phosphates with different chemical composition from aqueous solutions.

Experimental

Sorbents preparation

Phosphated dolomite $\text{Ca}_{0.7}\text{Mg}_{0.3}\text{HPO}_4 \cdot 2\text{H}_2\text{O}$ (PD-1) [27] and $\text{Ca}_{2.65}\text{Mg}_3(\text{NH}_4)_{1.3}(\text{PO}_4)_4(\text{CO}_3)_{0.3} \cdot 6\text{H}_2\text{O}$ (PD-2) [28] were used as starting materials for the preparation of Ti–Ca–Mg composite phosphates. Further, PD-1 or PD-2 samples was suspended in aqueous solution of titanyl-diammonium sulfate $(\text{NH}_4)_2\text{TiO}(\text{SO}_4)_2 \cdot \text{H}_2\text{O}$ with 3.85 wt% concentration without pH correction [29, 30] at various V/m ratios under constant stirring at a temperature of 25 °C for 24 h. Samples of Ti–Ca–Mg phosphates were obtained with a ratio of Ti/(Ca + Mg) in a reaction mixture of 10.0, 20.0, 33.0 and 60.0 wt% and marked as PD-1-1 (PD-2-1), PD-1-2 (PD-2-2), PD-1-3 (PD-2-3), PD-1-4 (PD-2-4), respectively [25].

Analytical methods

X-ray phase analysis of sorbents was performed at the ADVANCED8 facility (Bruker, Germany) using CuK_α radiation. Phase identification was performed using the base of radiographic powder standards “JCPDS PDF2”. The adsorption and texture properties were evaluated from low-temperature (–196 °C) physical adsorption–desorption of nitrogen isotherms performed on the surface area and porosity analyzer ASAP 2020 MP (Micromeritics, USA). The specific surface area was calculated by BET method (A_{BET}), sorption volume ($V_{\text{sp,des.}}$) and average pore diameter ($D_{\text{sp,des.}}$) was calculated by a single-point method on the desorption branch of isotherm. The relative error of determination was estimated at $\pm 1\%$ for pore volume and $\pm 15\%$ for the pore size and surface area.

Determination of the Ca, Mg, Ti and P content in the samples was performed by atomic emission spectroscopy with inductively coupled plasma on the Shimadzu ICPS-9000 mass spectrometer after conversion of the sorbents into solution using a mixture of concentrated nitric and hydrochloric acids. The content of NH_4^+ ions was determined by reverse titration with Nessler reagent. The content of S was determined by gravimetric method by precipitation of BaSO_4 .

Adsorption experiment with stable Cs⁺, Sr²⁺ and Co²⁺ ions

The sorption capacity towards Cs⁺, Sr²⁺ and Co²⁺ ions was determined under static conditions. The suspension of the sorbent 0.20 g was mixed with 50.0 mL of the model solution (pH 6.0) for 24 h until equilibrium was established. The optimal conditions for sorption experiment were chosen based on preliminary study [31]. Then sorbent was separated from the solution and the residual concentration of Cs⁺, Sr²⁺ and Co²⁺ was determined by atomic absorption spectrometry (Contr AA 300, Analytik Jena). The relative errors of the data were about 3%. Sorption capacity (q_e , mg g⁻¹) of Cs⁺, Sr²⁺ and Co²⁺ ions were calculated by following equation:

$$q_e = (C_0 - C_e) \times V/m \quad (1)$$

where C_0 , C_e —initial and equilibrium concentration, mg·dm⁻³; V —volume of solution, dm³; m —mass of sorbent, g.

Model solutions of 0.05 M Sr(NO₃)₂ and 0.05 M Co(NO₃)₂ were used for the determination of sorption capacity towards stable Sr²⁺ and Co²⁺. Aqueous solutions of CsCl with a concentration of 100 and 1000 mg·dm⁻³ were used for Cs⁺ sorption on PD-1 and PD-2 sample series, respectively. The reagents CsCl, Sr(NO₃)₂ and Co(NO₃)₂·6H₂O (Five Oceans Ltd., Belarus) without additional purification were used for solution preparation. The selection of concentrations of model solutions was carried out based on preliminary experiments.

Adsorption experiment with ¹³⁷Cs, ⁹⁰Sr and ⁶⁰Co radionuclides

To determine the sorption characteristics of samples in relation to ¹³⁷Cs, ⁹⁰Sr and ⁶⁰Co radionuclides, experiments were performed under static conditions by continuous mixing of a suspension of air-dry sorbent weighing about 0.050 or 0.100 g, weighted to an accuracy of 0.0001 g with 20.0 cm³ solution until equilibrium was established. Then the mixture was filtered through a paper filter “white tape” and specific activity of ¹³⁷Cs, ⁹⁰Sr and ⁶⁰Co radionuclides was determined in the filtrate. Based on the analysis results, the values of the distribution coefficient (K_d , cm³ g⁻¹) were calculated using Eq. (2):

$$K_d = \frac{A_0 - A_p}{A_p} \times \frac{V_p}{m_c} \quad (2)$$

where A_0 , A_p —initial and equilibrium specific activity, Bq dm⁻³; V —volume of solution, dm³; m —mass of sorbent, g.

The specific activity of ¹³⁷Cs, ⁹⁰Sr and ⁶⁰Co in solutions was determined by direct radiometric method using the SCS-50 M

spectrometric complex (Green Star Technologies, Russia), intrinsic relative error of 20%. Samples containing ⁹⁰Sr were kept for at least 14 days (5 half-lives of ⁹⁰Y) before measurement to establish the radioactive equilibrium of the ⁹⁰Sr-⁹⁰Y pair. During sorption of ¹³⁷Cs, model solutions containing 0.10 and 1.0 M NaNO₃, pH = 6.0, were used as the liquid phase. Before starting the experiments, ¹³⁷Cs radionuclide label was added to the solutions in an amount of about 10⁵ Bq dm⁻³. During sorption of ⁹⁰Sr, a model solution of 0.01 M CaCl₂ with pH = 6.0 was used as the liquid phase, in which indicator amounts of ⁹⁰Sr radionuclide for 10⁵ Bq dm⁻³ were introduced before the experiments. For ⁶⁰Co sorption tap water composition (in mg dm⁻³: Na⁺-6–8; K⁺-4–5; Mg²⁺-15–17; Ca²⁺-52–56; Cl⁻-6–8; SO₄²⁻-36–38; HCO₃⁻-200–205; total salinity-310–330; total hardness-3.6–3.8 mmol dm⁻³; pH = 7.5 ± 0.2) was used as liquid phase. Before the beginning of the experiments, indicator amounts of ⁶⁰Co radionuclide of about 10⁴ Bq dm⁻³ were introduced into the water and kept for 3 days to establish an equilibrium between the radioactive and inactive components of the solution.

To obtain comparative characteristics of the studied samples under similar conditions, sorption of ¹³⁷Cs, ⁹⁰Sr, ⁶⁰Co was carried out on the following industrial sorbents:

TiP: titanium phosphate [32] (Apatite, Russia);

TiSi: sodium–potassium titanosilicate [33] (Apatite, Russia);

KNiFeCN: nickel–potassium ferrocyanide supported on silica gel, TU 2641-003-51255813 -2007 (Moscow, Russia);

ZrNiFeCN: nickel ferrocyanide and zirconium hydroxide brand Thermoxide-35, TU 6200-305-12342266-98 (Sverdlovsk, Russia);

AlSi: the clinoptilolite of “Sokyrnytsia” deposition, TU U 14.5-00292540.001-2001 (Sokirnitsa, Ukraine).

MnO₂: manganese dioxide brand MDM, TU 2641-001-51255813-2007, (Moscow, Russia);

ZrO₂·TiO₂: titanium and zirconium hydrated dioxides brand Thermoxide-3K, TU 2641-014-12342266-04, (Sverdlovsk, Russia);

AC: activated wood crushed coal brand BAU GOST 6217-74 with specific surface area of 800 m² g⁻¹ and pore volume of 1.6 cm³ g⁻¹.

R-SO₃H: strongly acidic sulphocationite brand Tokem-140, (Kemerovo, Russia).

Results and discussion

Sorbent characterization

XRD data (Table 1) shows that the initial PD-1 sample is a mixture of well-crystallized calcium hydro

phosphates $\text{CaHPO}_4 \cdot 2\text{H}_2\text{O}$ and magnesium hydro phosphates $\text{MgHPO}_4 \cdot 3\text{H}_2\text{O}$ with a small content of dolomite $\text{CaMg}(\text{CO}_3)_2$. When interacting with titanyl ions, a small amount of calcium titanate CaTiO_3 and titanium oxyhydrate $\text{Ti}_{0.857}\text{O}_2\text{H}_{0.571}$ is detected. The formation of titanium phosphates is not detected by the XRD method, probably due to their amorphous nature. With an increase in the concentration of titanyl ions introduced into the reaction mixture in the preparation of mixed Ti–Ca–Mg phosphates, there is a decrease in the intensity of reflexes of the initial compounds, up to the formation of an amorphous product PD-1-4. According to the results of chemical analysis of mixed Ti–Ca–Mg phosphates, an increase in the concentration of titanyl ions in the reaction mixture is accompanied by an increase in the Ti content in the final products up to 16.8 wt%, and a simultaneous reduction of Mg from 4.31 to 0.35 wt%. This indicates the substitution of Mg atoms by Ti during the interaction of initial PD-1 sample with titanyl ions. The sulfur content in final products is due to the formation of slightly soluble calcium sulfate CaSO_4 , as a result of SO_4^{2-} ions interaction in the composition of titanium salt $(\text{NH}_4)_2\text{TiO}(\text{SO}_4)_2 \cdot \text{H}_2\text{O}$ and calcium hydrophosphate $\text{CaHPO}_4 \cdot 2\text{H}_2\text{O}$. The content of small amounts of NH_4^+ ions in mixed Ti–Ca–Mg phosphates, also due to their presence in the composition of titanyl-diammonium sulfate.

Only characteristic peaks of magnesium-ammonium phosphate $\text{MgNH}_4\text{PO}_4 \cdot 6\text{H}_2\text{O}$ are detected on the XRD

spectra of PD-2 sample, which together with the chemical analysis data indicates an amorphous state of the tertiary calcium $\text{Ca}_3(\text{PO}_4)_2$ and magnesium $\text{Mg}_3(\text{PO}_4)_2$ phosphates. An increase in the number of introduced titanyl ions is accompanied by a decrease in the intensity peaks of $\text{MgNH}_4\text{PO}_4 \cdot 6\text{H}_2\text{O}$ for PD-2-1 and PD-2-3 samples and the formation of an amorphous PD-2-4 sample. At the same time, there is decrease in the content of Mg atoms from 10.2 to 0.80 wt% and an increase in the content of Ti atoms to 17.1 wt%. This is in good agreement with the established fact of substitution of Mg atoms for Ti for samples of the PD-1 series. Attention is drawn to the almost constant content of NH_4^+ ions in all samples of PD-2 series, which is in the range of 3.0–4.0 wt%.

According to the data of low-temperature nitrogen adsorption–desorption (Table 2), Ti–Ca–Mg phosphates are mesoporous sorbents with IV type isotherms characteristic of this class of porous materials according to the IUPAC classification. As a result of the interaction of PD-1 sample with a titanyl-containing precursor, there is a significant increase in the specific surface characteristics from 11 to $232 \text{ m}^2 \text{ g}^{-1}$ and the sorption pore volume from 0.025 to $0.370 \text{ cm}^3 \text{ g}^{-1}$, as well as a decrease in the average pore size from 10.8 to 6.7 nm. At the same time, for all samples, the form of capillary-condensation hysteresis belongs to the H1 type, which is typical for adsorbents with cylindrical pores.

Table 1 Chemical and phase composition of mixed Ti–Ca–Mg phosphates

| Sample | Content of elements (wt%) | | | | | | Phase composition |
|--------|---------------------------|-------|-------|-------|-----------------|------|--|
| | Mg | Ca | Ti | P | NH_4^+ | S | |
| PD-1 | 4.31 | 16.75 | 0.00 | 18.54 | 0.00 | 0.00 | Major: $\text{CaHPO}_4 \cdot 2\text{H}_2\text{O}$, $\text{MgHPO}_4 \cdot 3\text{H}_2\text{O}$, Traces: $\text{CaMg}(\text{CO}_3)_2$ |
| PD-1-1 | 2.02 | 15.96 | 4.81 | 8.56 | 1.02 | 7.22 | Major: $\text{CaHPO}_4 \cdot 2\text{H}_2\text{O}$, $\text{MgHPO}_4 \cdot 3\text{H}_2\text{O}$, Traces: $\text{CaMg}(\text{CO}_3)_2$, CaSO_4 , CaTiO_3 , $\text{Ti}_{0.857}\text{O}_2\text{H}_{0.571}$ |
| PD-1-3 | 1.25 | 11.54 | 10.33 | 8.79 | 1.73 | 6.30 | Minor: CaTiO_3 , $\text{Ti}_{0.857}\text{O}_2\text{H}_{0.571}$ |
| PD-1-4 | 0.35 | 6.36 | 16.80 | 9.06 | 2.56 | 5.23 | Amorphous |
| PD-2 | 10.18 | 14.98 | 0.00 | 17.53 | 3.31 | 0.00 | Major: $\text{MgNH}_4\text{PO}_4 \cdot 6\text{H}_2\text{O}$ |
| PD-2-1 | 5.30 | 9.49 | 3.99 | 12.47 | 3.95 | 0.00 | Traces: $\text{MgNH}_4\text{PO}_4 \cdot 6\text{H}_2\text{O}$ |
| PD-2-3 | 3.23 | 7.70 | 10.01 | 11.02 | 3.32 | 1.42 | Traces: $\text{MgNH}_4\text{PO}_4 \cdot 6\text{H}_2\text{O}$ |
| PD-2-4 | 0.80 | 5.56 | 17.10 | 9.30 | 2.55 | 3.58 | Amorphous |

Table 2 Adsorption and textural characteristics of Ti–Ca–Mg phosphates

| Sample | Type of isotherm | Type of hysteresis loop | Specific surface area (A_{BET}) ($\text{m}^2 \text{ g}^{-1}$) | Pore volume ($V_{\text{sp,des}}$) ($\text{cm}^3 \text{ g}^{-1}$) | Pore size (D_{des}) (nm) |
|--------|------------------|-------------------------|--|--|-------------------------------------|
| PD-1 | IV | H1 | 11 | 0.025 | 10.8 |
| PD-1-1 | | H1 | 19 | 0.075 | 18.1 |
| PD-1-4 | | H1 | 232 | 0.370 | 6.7 |
| PD-2 | | H2 + H3 | 196 | 0.374 | 8.0 |
| PD-2-1 | | H3 | 100 | 0.286 | 12.0 |
| PD-2-4 | | H1 | 144 | 0.336 | 9.6 |

The change in adsorption characteristics for Ti–Ca–Mg phosphate samples based on PD-2 is extreme with a minimum of $100 \text{ m}^2 \text{ g}^{-1}$ specific surface area and a sorption pore volume of $0.286 \text{ cm}^3 \text{ g}^{-1}$ and a maximum of 12.0 nm average pore size for the PD-2-1 sample. This dependence of adsorption characteristics from the content of the input titanyl ions due to the change of porous structure formed of phosphates and is confirmed by the textural characteristics. In nitrogen adsorption–desorption isotherm of the initial sample PD-2 has a loop of capillary-condensation hysteresis of a hybrid-type H2 + H3 (the form of pores slit-like and wedge-shaped), which transformation in type H3 (form of long wedge-shaped) for sample PD-2-1 and then to type H1 (form of long cylindrical) for sample PD-2-4 (Table 2).

Adsorption behavior towards stable Cs(I), Sr(II) and Co(II) ions

The results of the effect of Ti content on the sorption capacity of mixed Ti–Ca–Mg phosphates towards stable Cs^+ , Sr^{2+} and Co^{2+} ions in aqueous solutions are presented in Figs. 1, 2 and 3 depends on Ti content in reaction mixture. The initial PD-1 sample practically does not sorb Cs^+ ions (the sorption capacity of 0.7 mg g^{-1}). The increase in the Ti content in the samples is accompanied by an increase in the sorption capacity to 12.6 mg g^{-1} for the PD-1-4 sample. The initial PD-2 sample on the contrary, is characterized by a high sorption capacity in relation to Cs^+ ions (176.3 mg g^{-1}) and with an increase in the Ti content more than $25.0 \text{ wt}\%$ there is a sharp decrease in sorption capacity to 35 mg g^{-1} . Thus, for a series of sorbents based on PD-2, the reverse dependence of the change in sorption capacity towards Cs^+ ions is observed in comparison with samples obtained from PD-1. Thus, the obtained data on the increase in sorption capacity with an increase in the content of titanium are due

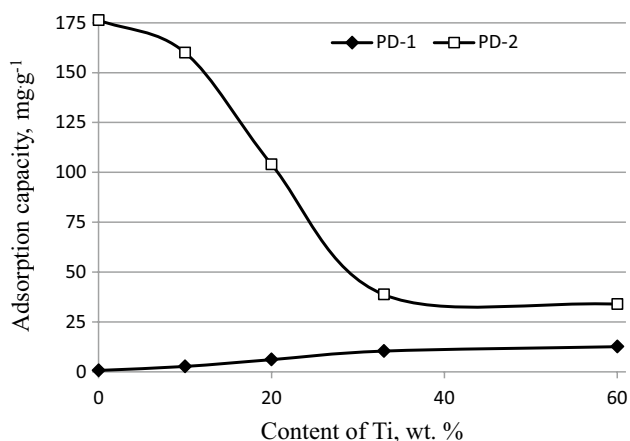


Fig. 1 Effect of Ti content in a reaction mixture on the adsorption capacity for Ca–Mg–Ti phosphate sorbents towards stable Cs^+ ions

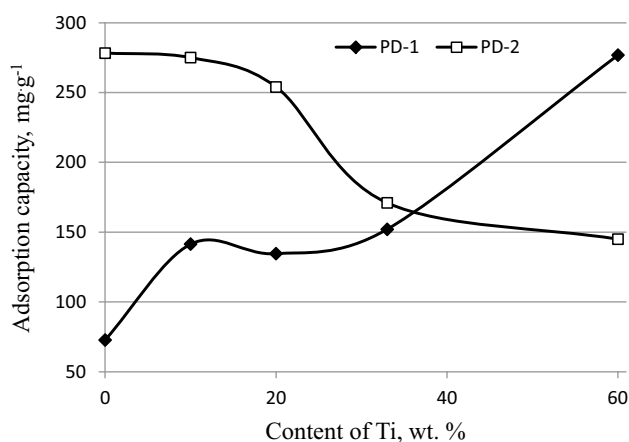


Fig. 2 Effect of Ti content in a reaction mixture on the adsorption capacity for Ca–Mg–Ti phosphate sorbents towards stable Sr^{2+} ions

to the formation of a phase of titanium hydrophosphate, which is characterized by a high ion exchange capacity and selectivity towards Cs^+ ions [26, 29, 30].

Similar patterns are observed in the sorption of stable Sr^{2+} ions. Thus, an increase in the Ti content in the samples of the PD-1 series leads to an increase in the sorption capacity of Sr^{2+} ions from 68 to 275 mg g^{-1} , and at the same time for sorbents obtained from PD-2, there is a decrease in the capacity from 275 to 150 mg g^{-1} (Fig. 2). This indicates a positive effect of the introduction of titanyl ions in the composition of Ca–Mg hydrophosphates (PD-1) on their sorption properties towards stable Cs^+ and Sr^{2+} ions. Contrary, a negative effect in the case of sorbents obtained from a mixture of tertiary Ca–Mg phosphates (PD-2). It has been shown that both magnesium phosphates and calcium phosphates are involved in the Sr^{2+} ions sorption processes: MgHPO_4 is the most active

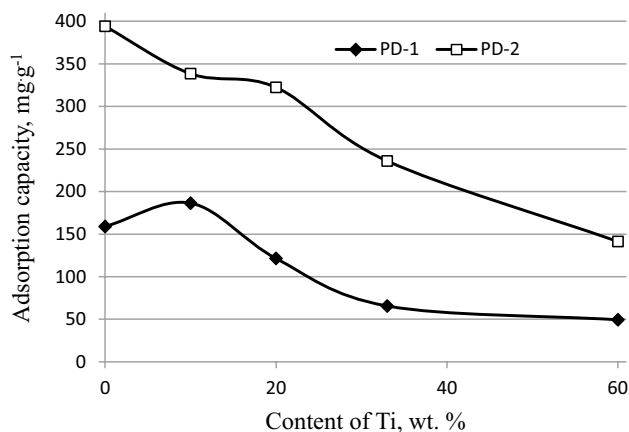


Fig. 3 Effect of Ti content in a reaction mixture on the adsorption capacity for Ti–Ca–Mg phosphate sorbents towards stable Co^{2+} ions

component in the PD-1 sample, $\text{MgNH}_4\text{PO}_4 \cdot 6\text{H}_2\text{O}$ along with $\text{Ca}_3(\text{PO}_4)_2$ makes a significant contribution to the sorption of Sr(II) by the PD-2 sample [17]. It could be a main reason of different sorption activity of prepared Ti–Ca–Mg phosphate sorbents towards Sr^{2+} ions.

The sorption efficiency of stable Co^{2+} ions are the same for PD-1 and PD-2 series samples. The initial Ca–Mg phosphates without Ti are characterized by a higher sorption capacity towards Co^{2+} ion, the capacity is reduced from 400 and 160 mg g^{-1} to 60 and 150 mg g^{-1} for the PD-1 and PD-2 series, respectively (Fig. 3). This indicates a negative effect of the introduction of titanyl ions in the composition of the initial Ca–Mg phosphates PD-1 and PD-2 on their sorption properties towards Co^{2+} ions. Ca–Mg phosphates with a different phase composition were studied as effective sorbents for ^{60}Co removal from high salinity water. It was shown that the chemical reaction of Ca–Mg phosphates with Co^{2+} ions leads to the effective removal of ^{60}Co radionuclide [19]. Thus, the formation of titanium phosphate during substitution of calcium and magnesium ions of PD-1 and PD-2 samples leads to decreasing of sorption capacity obtained Ti–Ca–Mg phosphate sorbents towards Co^{2+} ions.

Thus, mixed Ti–Ca–Mg phosphates for the PD-1 and PD-2 series form the inverse series (3) and (4) for the sorption capacity towards stable Cs^+ and Sr^{2+} ions:

$$\text{PD-1} < \text{PD-1-1} < \text{PD-1-2} < \text{PD-1-3} < \text{PD-1-4} \quad (3)$$

$$\text{PD-2} < \text{PD-2-1} < \text{PD-2-2} < \text{PD-2-3} < \text{PD-2-4} \quad (4)$$

At the same time, in the second sorption capacity for Co^{2+} ion, the sorbents are arranged in a following row:

$$\text{PD-1(PD-2)} > \text{PD-1(PD-2)-1} > \text{PD-1(PD-2)-2} > \text{PD-1(PD-2)-3} > \text{PD-1(PD-2)-4} \quad (5)$$

It can be concluded that the sorption capacity of mixed Ti–Ca–Mg towards stable Cs^+ , Sr^{2+} and Co^{2+} ions is mainly determined by their chemical composition. At the same time, the adsorption and textural characteristics of the studied sorbents practically do not affect their sorption capacity towards stable ions from aqueous solutions. This is probably due to the ion exchange mechanism Cs^+ and Sr^{2+} ions of adsorption and by chemisorption process for Co^{2+} ions, which is consistent with established patterns.

Adsorption characteristics toward ^{137}Cs , ^{90}Sr and ^{60}Co radionuclides

The results of the sorption activity of prepared phosphate sorbents towards ^{137}Cs , ^{90}Sr and ^{60}Co radionuclides are presented in Table 3. To study the radionuclides sorption the initial samples of PD-1 and PD-2 and mixed Ti–Ca–Mg phosphates PD-1-3 and PD-1-4, as well as PD-2-2 and PD-2-4 were selected.

The results of ^{137}Cs radionuclide sorption correspond to the previously obtained data on stable Cs^+ ions—the introduction of Ti in the composition of PD-1 causes an increase in K_d ^{137}Cs on the background of 0.1 M NaNO_3 from 0.48×10^3 to $(1.63\text{--}1.36) \times 10^3 \text{ cm}^3 \text{ g}^{-1}$. It indicates an increase in the affinity of mixed Ti–Ca–Mg phosphates based on PD-1 to ^{137}Cs radionuclide. A similar relationship is observed for samples of the PD-2 series: with an increase in the Ti content in the sorbents, an increase in K_d ^{137}Cs is accompanied by an increase from 0.08×10^3 to $(0.82\text{--}0.89) \times 10^3 \text{ cm}^3 \text{ g}^{-1}$. It is important to note that the initial PD-2 sample shows low affinity towards ^{137}Cs radionuclide. It is fully inconsistent with the sorption capacity data obtained for stable Cs^+ ions. At the same time, the highest selective sorption properties are characterized by PD-1-3 and PD-1-4 samples obtained based on PD-1. It does not correlate with data on the sorption capacity of stable Cs^+ ions (Fig. 1). The possible explanation of such contradictory results of stable and radioactive cesium sorption is the following. Uptake of stable Cs^+ in solution without competing ions corresponds to the measured textural characteristics of both sorbents (Table 2). High selectivity of titanium

hydrophosphate phase plays the minor role as the number of binding sites of this phase is rather small comparing to total number of binding sites that limits the adsorption capacity. For ^{137}Cs with Na^+ background the estimated Na:Cs atoms ratio in solution is more than 10^8 so almost all binding sites of starting sorbents of PD-1 and PD-2 series are occupied by Na^+ , resulting in low K_d values of ^{137}Cs . In this case the introduction of highly selective towards cesium ions titanium hydrophosphate phase significantly increases ^{137}Cs K_d

Table 3 Adsorption characteristics of Ti–Ca–Mg phosphates towards ^{137}Cs , ^{90}Sr and ^{60}Co radionuclides ($K_d \times 10^3, \text{cm}^3 \text{ g}^{-1}$)

| Radionuclide | Competition ions | Sample | | | | | |
|-------------------|------------------------|--------|--------|--------|------|--------|--------|
| | | PD-1 | PD-1-3 | PD-1-4 | PD-2 | PD-2-2 | PD-2-4 |
| ^{137}Cs | 0.1 M NaNO_3 | 0.48 | 1.63 | 1.36 | 0.08 | 0.82 | 0.89 |
| | 1.0 M NaNO_3 | 0 | 0.08 | 0.43 | 0 | 0.14 | 0.18 |
| ^{90}Sr | 0.01 M CaCl_2 | 0.28 | 0.57 | 0.18 | 1.50 | 4.20 | 0.67 |
| ^{60}Co | Tap water | 3.60 | 0.05 | 0.06 | 2.30 | 1.40 | 0.10 |

Table 4 Comparison adsorption characteristics of Ti–Ca–Mg phosphates with other materials

| | Sample | $K_d \times 10^3 \text{ (cm}^3 \text{ g}^{-1}\text{)}$ | | | | | |
|-------------------|--------------------------|--|--------|--------|---------|------------------------------------|------------------|
| | | PD-1-4 | TiP | TiSi | KNiFeCN | ZrNiFeCN | AlSi |
| ^{137}Cs | 0.1 M NaNO ₃ | 1.36 | 2.20 | 46.0 | 84.0 | 120 | 2.10 |
| | 1.0 M NaNO ₃ | 0.43 | 0.15 | 41.0 | 73.0 | 81.0 | 0.12 |
| | Sample | PD-2 | PD-2-2 | TiP | TiSi | ZrO ₂ ·TiO ₂ | MnO ₂ |
| ^{90}Sr | 0.01 M CaCl ₂ | 1.50 | 4.20 | 46.0 | 35.0 | 0.22 | 86.0 |
| | Sample | PD-1 | PD-2 | PD-2-2 | AC | R-SO ₃ H | |
| ^{60}Co | Tap water | 3.60 | 2.30 | 1.40 | 4.90 | 4.30 | |

for all Ca–Mg–Ti sorbents PD-1-3, PD-1-1, PD-2-2, PD-2-4. The dependence of ^{137}Cs on background Na⁺ concentration is the additional evidence for selectivity being the driven factor of ^{137}Cs sorption.

The change in the affinity of the Ti–Ca–Mg phosphates towards ^{90}Sr radionuclide against a background of 0.01 M CaCl₂ has an extreme dependence on the composition of sorbents with a maximum K_d for PD-1-1 of ($0.57 \times 10^3 \text{ cm}^3 \text{ g}^{-1}$) and PD-2-2 ($4.20 \times 10^3 \text{ cm}^3 \text{ g}^{-1}$) samples with a Ti content of 7.0 and 15.0 wt%, respectively. This extreme change in K_d ^{90}Sr depends on Ti content is not correlated with a monotonous increase or decrease in the sorption capacity of Sr²⁺ ions for samples of PD-1 and PD-2 series, respectively (Fig. 2). At the same time, the relative affinity of similar sorbents of PD-1 and PD-2 series towards ^{90}Sr radionuclide is in good agreement with the data on sorption capacity of stable Sr²⁺ ions.

The presented results of ^{60}Co radionuclide sorption show that the highest affinity has samples that do not contain or contain minimal amounts of Ti (PD-1, PD-2 and PD-2-2), which is quite correlated with a monotonous decrease in sorption capacity for stable Co²⁺ ions (Fig. 3). The highest values of K_d for ^{60}Co reach 3.60×10^3 and $2.30 \times 10^3 \text{ cm}^3 \text{ g}^{-1}$ for the initial Ca–Mg phosphates PD-1 and PD-2, respectively (Table 3).

Different trends in sorption activity in relation to radionuclides and stable ions depending on the composition of sorbents clearly indicates significant differences in the mechanisms of adsorption of macro and micro quantities of ions. Moreover, these processes depend not only on the composition of the sorbent, but also on the nature of the radionuclide and are not predictable enough based on stable ions sorption results. It requires mandatory studies of the effectiveness of sorbents using model solutions of radionuclides.

Comparison study with other materials

Table 4 compares the adsorption characteristics of the obtained mixed phosphates with the known most effective

sorbents for individual radionuclides. Mixed Ti–Ca–Mg phosphates are inferior in efficiency of adsorption of ^{137}Cs radionuclide by KNiFeCN ferrocyanide ($84.0 \times 10^3 \text{ cm}^3 \text{ g}^{-1}$) and ZrNiFeCN ($120 \times 10^3 \text{ cm}^3 \text{ g}^{-1}$) and titanosilicate TiSi ($46.0 \times 10^3 \text{ cm}^3 \text{ g}^{-1}$) sorbents, which are the most effective of the currently known in relation to these radionuclides. At the same time, they are characterized by comparable K_d values in the range of ($1.36\text{--}2.20$) $\times 10^3 \text{ cm}^3 \text{ g}^{-1}$ in comparison with titanium phosphate TiP and aluminosilicate AlSi. The AlSi, TiSi and KNiFeCN sorbents showed the highest sorption efficiency towards ^{90}Sr radionuclide with K_d in the range of ($35.0\text{--}86.0$) $\times 10^3 \text{ cm}^3 \text{ g}^{-1}$. At the same time, PD-2 and PD-2-2 samples are also characterized by high affinity for radionuclide ^{90}Sr for which K_d is 1.50×10^3 and $4.20 \times 10^3 \text{ cm}^3 \text{ g}^{-1}$, respectively. All studied samples have a close affinity for the radionuclide ^{60}Co — K_d varies from 1.40×10^3 to $4.30 \times 10^3 \text{ cm}^3 \text{ g}^{-1}$.

The obtained phosphate sorbents are characterized by lower K_d values compared to the materials used for the removal of individual radionuclides, both studied in this work and described in the literature [34–38]. However, depending on the composition of mixed Ti–Ca–Mg phosphates, it is possible to obtain sorbents characterized by high affinity for all three radionuclides ^{137}Cs , ^{90}Sr and ^{60}Co . This allows them to be considered as promising materials for one-stage purification of LRW complex chemical and radionuclide composition.

Conclusions

Sorption characteristics of mixed Ti–Ca–Mg phosphates were studied on model solutions of stable and radioactive Cs(I), Sr(II) and Co(II) ions. It was found that double Ca–Mg phosphates PD-1 ($q \text{ Cs}^+ 175 \text{ mg g}^{-1}$) and PD-2 ($q \text{ Sr}^{2+} 275 \text{ mg g}^{-1}$ and $q \text{ Co}^{2+} 380 \text{ mg g}^{-1}$) are characterized by the highest sorption capacity in relation to stable ions. Sorbents based on mixed Ti–Ca–Mg phosphates PD-1-3, PD-2-2 and PD-1 are characterized by the highest values of

distribution coefficients in relation to radionuclides ^{137}Cs ($1.63 \times 10^3 \text{ cm}^3 \text{ g}^{-1}$), ^{90}Sr ($4.20 \times 10^3 \text{ cm}^3 \text{ g}^{-1}$) and ^{60}Co ($3.60 \times 10^3 \text{ cm}^3 \text{ g}^{-1}$), respectively. The established differences in the sorption of macro quantities of stable Cs^+ , Sr^{2+} and Co^{2+} ions and micro concentrations of ^{137}Cs , ^{90}Sr and ^{60}Co radionuclides have to be taken into account for evaluation of the effectiveness of sorbents for the real liquid radioactive waste treatment. Depending on the composition of the mixed Ti–Ca–Mg phosphates, it is possible to obtain materials with high affinity for all three radionuclides ^{137}Cs , ^{90}Sr and ^{60}Co and comparable characteristics with industrial sorbents.

Funding This study was supported by Belarusian state program of scientific research (Grant No. 1.05).

References

1. Yasunari TJ, Stohl A, Hayano RS, Burkhart JF, Eckhardt S, Yasunari T (2011) Cesium-137 deposition and contamination of Japanese soils due to the Fukushima nuclear accident. *Proc Natl Acad Sci USA* 108(49):19530–19534. <https://doi.org/10.1073/pnas.1112058108>
2. Mertz JL, Fard ZH, Malliakas CD, Manos MJ, Kanatzidis MG (2013) Selective removal of Cs^+ , Sr^{2+} , and Ni^{2+} by $\text{K}_{2x}\text{Mg}_x\text{Sn}_{3-x}\text{S}_6$ ($x = 0.5-1$) (KMS-2) relevant to nuclear waste remediation. *Chem Mater* 25(10):2116–2127. <https://doi.org/10.1021/cm400699r>
3. Aguila B, Banerjee D, Nie ZM, Shin Y, Ma SQ, Thallapally PK (2016) Selective removal of cesium and strontium using porous frameworks from high level nuclear waste. *Chem Commun* 52(35):5940–5942. <https://doi.org/10.1039/c6cc00843g>
4. Ivanets AI, Shashkova IL, Kitikova NV, Drozdova NV (2014) Extraction of Co(II) ions from aqueous solutions with thermally activated dolomite. *Russ J Appl Chem* 87:270–275. <https://doi.org/10.1134/S1066362214050129>
5. Abdel-Rahman RO, El-Kamash AM, Ali HF, Hong YT (2011) Overview on recent trends and developments in radioactive liquid waste treatment. Part 1: sorption/ion exchange technique. *Int J Environ Eng Sci* 2:1–16
6. Narbutt J, Bilewicz A, Bartoś B (1994) Composite ion exchangers. Prospective nuclear applications. *J Radioanal Nucl Chem* 183:27–32. <https://doi.org/10.1007/BF02043113>
7. Bilewicz A, Narbutt J (2001) α -Crystalline polyantimonic acid: an adsorbent for radiostrontium, and a potential primary barrier in waste repositories. *Radiochim Acta* 89:783–784. <https://doi.org/10.1524/ract.2001.89.11-12.783>
8. Chon K, Kim SJ, Moon J, Cho J (2012) Combined coagulation-disk filtration process as a pretreatment of ultrafiltration and reverse osmosis membrane for wastewater reclamation: an autopsy study of a pilot plant. *Water Res* 46(6):1803–1816. <https://doi.org/10.1016/j.watres.2011.12.062>
9. Montaña M, Camacho A, Serrano I, Devesa R, Matia L, Vallés I (2013) Removal of radionuclides in drinking water by membrane treatment using ultrafiltration, reverse osmosis and electrodialysis reversal. *J Environ Radioact* 125:86–92. <https://doi.org/10.1016/j.jenvrad.2013.01.010>
10. Rat'ko AI, Ivanets AI, Sakhar IO, Davydov DYU, Toropova VV, Radkevich AV (2011) A sorbent based on natural dolomite for recovery of cobalt radionuclides. *Radiochemistry*. <https://doi.org/10.1134/S1066362211060105>
11. Mou J, Wang G, Shi W, Zhang S (2012) Sorption of radiocobalt on a novel $\gamma\text{-MnO}_2$ hollow structure: effects of pH, ionic strength, humic substances and temperature. *J Radioanal Nucl Chem*. <https://doi.org/10.1007/s10967-011-1408-0>
12. Kitikova NV, Ivanets AI, Shashkova IL, Radkevich AV, Shemet LV, Kul'bitskaya LV, Sillanpää M (2017) Batch study of ^{85}Sr adsorption from synthetic seawater solutions using phosphate sorbents. *J Radioanal Nucl Chem* 314(3):2437–2447. <https://doi.org/10.1007/s10967-017-5592-4>
13. Rashad GM, Mahmoud MR, Elewa AM, Metwally E, Saad EA (2016) Removal of radiocobalt from aqueous solutions by adsorption onto low-cost adsorbents. *J Radioanal Nucl Chem*. <https://doi.org/10.1007/s10967-016-4726-4>
14. Ryabchikov BE (2008) Decontamination of liquid radioactive wastes. De Li, Moscow
15. Shashkova IL, Ivanets AI, Kitikova NV (2019) Sorption of Co^{2+} , Pb^{2+} , and Sr^{2+} ions on hydroxyapatite, synthesized in the presence of oxyethylenediphosphonic acid. *Russ J Appl Chem* 92(5):625–633. <https://doi.org/10.1134/S1070427219050070>
16. Milenkovic AS, Smiciklas ID, Sljivic-Ivanovic MZ, Zivkovic LS, Vukelic NS (2016) Effect of experimental variables onto Co^{2+} and Sr^{2+} sorption behavior in red mud-water suspensions. *J Environ Sci Health A*. <https://doi.org/10.1080/10934529.2016.1159884>
17. Shashkova IL, Ivanets AI, Kitikova NV, Sillanpää M (2017) Effect of phase composition on sorption behavior of Ca-Mg phosphates towards Sr(II) ions in aqueous solution. *J Taiwan Inst Chem Eng*. <https://doi.org/10.1016/j.jtice.2017.09.027>
18. Luca V, Bianchi HL, Manzini AC (2012) Cation immobilization in pyrolyzed simulated spent ion exchange resins. *J Nucl Mater*. <https://doi.org/10.1016/j.jnucmat.2012.01.004>
19. Ivanets A, Kitikova N, Shashkova I, Radkevich A, Shemet L, Sillanpää M (2018) Effective removal of ^{60}Co from high-salinity water by Ca–Mg phosphate sorbents. *J Radioanal Nucl Chem* 318(3):2341–2347. <https://doi.org/10.1007/s10967-018-6291-5>
20. Avramenko VA, Egorin AM, Papynov EK, Sokol'nitskaya TA, Tananaev IG, Sergienko VI (2017) Processes for treatment of liquid radioactive waste containing seawater. *Radiochemistry* 59:407–413. <https://doi.org/10.1134/S1066362217040142>
21. Ivanets AI, Prozorovich VG, Kouznetsova TF, Radkevich AV, Krivoschapkin PV, Krivoschapkina EF, Sillanpää M (2018) Sorption behavior of ^{85}Sr onto manganese oxides with tunnel structure. *J Radioanal Nucl Chem* 316:673–683. <https://doi.org/10.1007/s10967-018-5771-y>
22. Milyutin VV, Nekrasova NA, Yanicheva NY, Kalashnikova GO, Ganicheva YY (2017) Sorption of cesium and strontium radionuclides onto crystalline alkali metal titanates. *Radiochemistry* 59:65–69. <https://doi.org/10.1134/S1066362217010088>
23. Denecke MA, Bryan N, Bryn N, Kalmykov S, Morris K, Quinto F (2018) Sources and behaviour of actinide elements in the environment. *Exp Theor Approach Actin Chem*. <https://doi.org/10.1002/9781119115557.ch8>
24. Ivanets AI, Prozorovich VG, Kouznetsova TF, Radkevich AV, Zarubo AM (2016) Mesoporous manganese oxides prepared by sol-gel method: synthesis, characterization and sorption properties towards strontium ions. *Environ Nanotechnol Monit Manag* 6:261–269. <https://doi.org/10.1016/j.enmm.2016.11.004>
25. Ivanets AI, Shashkova IL, Kitikova NV, Maslova MV, Mudruk NV (2019) New heterogeneous synthesis of mixed Ti–Ca–Mg phosphates as efficient sorbents of ^{137}Cs , ^{90}Sr and ^{60}Co radionuclides. *J Taiwan Inst Chem Eng* 104:151–159. <https://doi.org/10.1016/j.jtice.2019.09.001>
26. Maslova M, Mudruk N, Ivanets A, Shashkova I, Kitikova N (2020) A novel sorbent based on Ti–Ca–Mg phosphates: synthesis,

- characterization, and sorption properties. *Environ Sci Pollut Res* 27:3933–3949. <https://doi.org/10.1007/s11356-019-06949-3>
27. Ivanets AI, Srivastava V, Kitikova NV, Shashkova IL, Sillanpää M (2017) Non-apatite Ca-Mg phosphate sorbent for removal of toxic metal ions from aqueous solutions. *J Environ Chem Eng* 5:2010–2017. <https://doi.org/10.1016/j.jece.2017.03.041>
28. Ivanets AI, Kitikova NV, Shashkova IL, Oleksienko OV, Levchuk I, Sillanpää M (2014) Removal of Zn^{2+} , Fe^{2+} , Cu^{2+} , Pb^{2+} , Cd^{2+} , Ni^{2+} and Co^{2+} ions from aqueous solutions using modified phosphate dolomite. *J Environ Chem Eng* 2(2):981–987. <https://doi.org/10.1016/j.jece.2014.03.018>
29. Maslova MV, Gerasimova LG (2011) The influence of chemical modification on structure and sorption properties of titanium phosphate. *Russ J Appl Chem* 84:1–8
30. Maslova MV, Ivanenko VI, Gerasimova LG, Ryzhuk NL (2018) Effect of synthesis method on the phase composition and ion-exchange properties of titanium phosphate. *Russ J Inorg Chem* 63:1141–1148. <https://doi.org/10.1134/S0036023618090115>
31. Ivanets A, Kitikova N, Shashkova I, Radkevich A, Stepanchuk T, Maslova M, Mudruk N (2020) One-stage adsorption treatment of liquid radioactive wastes with complex radionuclide composition. *Water Air Soil Pollut* 231(4):1–10. <https://doi.org/10.1007/s11270-020-04529-7>
32. Maslova MV, Rusanova D, Naydenov V, Antzutkin ON, Gerasimova LG (2012) Extended study on the synthesis of amorphous titanium phosphates with tailored sorption properties. *J Non-Cryst Solids* 358:2943–2950. <https://doi.org/10.1016/j.jnoncrysol.2012.06.033>
33. Maslova MV, Rusanova D, Naydenov V, Antzutkin ON, Gerasimova LG (2008) Synthesis, characterization, and sorption properties of amorphous titanium phosphate and silica-modified titanium phosphates. *Inorg Chem* 47:11351–11360. <https://doi.org/10.1021/ic801274z>
34. Zhao D, Wang Y, Xuan H, Chen Y, Cao T (2013) Removal of radiocobalt from aqueous solution by Mg_2Al layered double hydroxide. *J Radioanal Nucl Chem*. <https://doi.org/10.1007/s10967-012-1994-5>
35. Pshinko GN, Puzyrnaya LN, Shunkov VS, Kosorukov AA, Demchenko VY (2016) Removal of cesium and strontium radionuclides from aqueous media by sorption onto magnetic potassium zinc hexacyanoferrate (II). *Radiochemistry*. <https://doi.org/10.1134/S1066362216050088>
36. Egorin A, Sokolnitskaya T, Azarova Y, Portnyagin A, Balanov M, Misko D, Shelestyuk E, Kalashnikova A, Tokar E, Tananaev I, Avramenko V (2018) Investigation of Sr uptake by birnessite-type sorbents from seawater. *J Radioanal Nucl Chem* 317:243–251. <https://doi.org/10.1007/s10967-018-5905-2>
37. Guo Z, Ling Q, Zhou Y, Wei L, Zhou R, Niu H, Li Y, Xu J (2017) Synthesis of three-dimensional flower-like $\alpha-Fe_2O_3$ microspheres for high efficient removal of radiocobalt. *J Radioanal Nucl Chem*. <https://doi.org/10.1007/s10967-017-5534-1>
38. Semenichev VS, Voronina AV, Bykov AA (2013) The study of sorption of cesium radionuclides by “T-55” ferrocyanide sorbent from various types of liquid radioactive wastes. *J Radioanal Nucl Chem* 295:1753–1757. <https://doi.org/10.1007/s10967-012-2299-4>

Publisher's Note Springer Nature remains neutral with regard to jurisdictional claims in published maps and institutional affiliations.